BMB Reports - Manuscript Submission

Manuscript Draft

Manuscript Number: BMB-16-182

Title: Effects of Chlorogenic Acid on Intracellular Calcium Regulation in Lysophosphatidylcholine-Treated Endothelial Cells

Article Type: Article

Keywords: Chlorogenic acid; Calcium; Lysophosphatidylcholine; Store-operated channel; Transient receptor potential canonical channel 1

Corresponding Author: Jae-Hoon Bae

Authors: Hye-Jin Jung[1,#], Seung-Soon Im[1,#], Dae-Kyu Song[1], Jae-Hoon Bae[1,*]

Institution: [1]Physiology, Keimyung University School of Medicine,

Effects of Chlorogenic Acid on Intracellular Calcium Regulation in Lysophosphatidylcholine-Treated Endothelial Cells

Hye-Jin Jung[1], Seung-Soon Im[1], Dae-Kyu Song, Jae-Hoon Bae*

Department of Physiology, Keimyung University School of Medicine, 1095 Dalgubeol-Daero, Dalseo-Gu, Daegu 704-701, South Korea

Running Title: Role of chlorogenic acid in LPC-treated HUVECs

[1] These authors contributed equally to this work.

Corresponding author:

Department of Physiology, Keimyung University School of Medicine, 1095 Dalgubeol-Daero, Dalseo-Gu, Daegu 704-701, South Korea.

E-mail address: jhbae@dsmc.or.kr (J.-H. Bae).

Tel.: +82-53-580-3872

Fax: +82-53-580-3793

ABSTRACT

Lysophosphatidylcholine (LPC) is a major phospholipid component of oxidized low-density lipoprotein (ox-LDL) and is implicated in its atherogenic activity. This study investigated the effects of LPC on cell viability, intracellular calcium homeostasis, and the protective mechanisms of chlorogenic acid (CGA) in human umbilical vein endothelial cells (HUVECs). LPC increased intracellular calcium ($[Ca^{2+}]_i$) by releasing Ca^{2+} from intracellular stores and via Ca^{2+} influx through store-operated channels (SOCs). LPC also increased the generation of reactive oxygen species (ROS) and decreased cell viability. The mRNA expression of Transient receptor potential canonical (TRPC) channel 1 was increased significantly by LPC treatment and suppressed by CGA. CGA inhibited LPC-induced Ca^{2+} influx and ROS generation, and restored cell viability. These results suggested that CGA inhibits SOC-mediated Ca^{2+} influx and ROS generation by attenuating *TRPC1* expression in LPC-treated HUVECs. Therefore, CGA might protect endothelial cells against LPC injury, thereby inhibiting atherosclerosis.

Keywords: Chlorogenic acid, Calcium, Lysophosphatidylcholine, Store-operated channel, Transient receptor potential canonical channel 1

Abbreviations

CGA, chlorogenic acid; ER, endoplasmic reticulum; Fura-2/AM, fura-2 acetoxymethyl; DPI, diphenyleneiodonium; GA-1000, gentamicin sulfate amphotericin-B; GAPDH, glyceraldehyde-3-phosphate dehydrogenase; Gd^{3+}, gadolinium; HUVEC, human umbilical vein endothelial cell; IP3, 1,4,5-tris-phosphate; La^{3+}, lanthanum; LDL, low-density lipoprotein; LPC, Lysophosphatidylcholine; MTT, 3-(4,5-dimethylthiazol- 2-yl)-2,5-diphenyltetrazolium bromide; NAC, N-acetyl-L-cysteine; PLC, phospholipase C; ROS, reactive oxidative species; SOC, store-operated channel; TRP, transient receptor potential; TRPC, transient receptor potential channel.

INTRODUCTION

Lysophosphatidylcholine (LPC) is generated by the hydrolysis of phosphatidylcholine by phospholipase A2, and 1-palmitoyl-sn-glycero-3-phosphocholine is the main component of phospholipids. LPC is a major component of oxidized low-density lipoprotein (ox-LDL), which causes atherosclerosis (1). LPC induces endothelial cell dysfunction by generating reactive oxygen species (ROS) in the vascular endothelium and increases oxidative stress by increasing the free Ca^{2+} concentration in the cytoplasm of leukocytes, macrophages, and muscle cells (2). Intracellular calcium ions (Ca^{2+}) are important secondary messengers and mediators of signal transduction in cells (3), which play important roles in various physiological processes and metabolic signaling (4). Usually, the intracellular Ca^{2+} concentration ($[Ca^{2+}]_i$) is low at 100 nmol/L, and this is maintained by protein binding or movement through ion channels (5). If the $[Ca^{2+}]_i$ is increased by specific stimulation, cellular responses, including inflammation, cell growth, cell proliferation, thrombosis, oxidative stress, and calcification, can occur (6). The increase in $[Ca^{2+}]_i$ induced by LPC is observed in various cell types associated with atherosclerosis and inflammatory diseases, such as endothelial cells, monocytes, macrophages, and myocardial cells (7). LPC increases $[Ca^{2+}]_i$ through store-operated Ca^{2+} channels (SOC) in various cells. Functional analysis via mRNA expression of transient receptor potential canonical (TRPC) channels has led to it being identified as a molecular component of SOC (8).

Chlorogenic acid (CGA) is a polyphenol that is abundant in *Crataegus monogyna*, *Eucalyptus globules*, *Eupatorium perfoliatum*, *Vaccinium angustifolium*, and, especially, coffee (8-11). CGA is one of the many powerful phenolic antioxidant compounds in coffee (12). CGA has myocardial protective effects via the inhibition of lipid peroxidation, has anti-tumor effects, and produces antioxidant effects by removing free radicals (13). Dietary CGA also improves endothelial cell dysfunction by reducing the free radical generation of nitric oxide (12).

In this study, we demonstrated the function of LPC in $[Ca^{2+}]_i$-induced cell damage and investigated the protective effects of CGA against oxidative stresses in human umbilical vein endothelial cells (HUVECs).

RESULTS

Effect of CGA on LPC-induced reductions in cell viability

To determine the cytotoxic effects of LPC, cell viability was measured in HUVECs using the MTT (3-(4,5-dimethylthiazol- 2-yl)-2,5-diphenyltetrazolium bromide) assay. Treatment with LPC (10–100 μmol/L) for 1 h reduced cell viability significantly in a dose-dependent manner (Fig. 1A). CGA was then assessed for its inhibitory effect on LPC-induced cytotoxicity in HUVECs. The cytotoxic effect of LPC (30 μmol/L) challenge for 1 h was blocked by pretreatment with CGA (100–1000 μmol/L) for 24 h. Moreover, at CGA concentrations greater than 300 μmol/L, the blocking effect was marked (Fig. 1B). We also observed the effect of CGA treatment without LPC on the HUVECs' viability. CGA increased the cell viability significantly compared with vehicle-treated control cells after 24 h of incubation (Fig. 1C). These results indicated that CGA could ameliorate the LPC-induced reduction in cell viability.

Intracellular Ca^{2+} concentration changes after LPC treatment

To investigate the effect of LPC on changes in $[Ca^{2+}]_i$ in HUVECs, $[Ca^{2+}]_i$ was measured in the cells before and after LPC treatment. $[Ca^{2+}]_i$ increased with increasing concentrations of LPC (10–50 μmol/L), administered with physiological saline solution (PSS) containing 1.8 mmol/L Ca^{2+} (Fig. 2A). To determine whether the increased $[Ca^{2+}]_i$ was caused by Ca^{2+} release from the endoplasmic reticulum (ER), $[Ca^{2+}]_i$ was measured after blocking Ca^{2+} secretion from the ER. The increase in $[Ca^{2+}]_i$ induced by LPC was suppressed by ER inhibitors (Fig. 2B). To assess the effect of CGA on the increased $[Ca^{2+}]_i$ induced by LPC, changes in Ca^{2+} concentration after LPC

(50 μmol/L) challenge, following pretreatment with CGA (300-1000 μmol/L), were measured. CGA inhibited both Ca^{2+} release from the ER and intake from outside the cells in a dose-dependent manner (Fig. 2C). The effect of CGA treatment without LPC on $[Ca^{2+}]_i$ was tested in the presence and absence of external Ca^{2+}. CGA alone did not cause any significant changes in $[Ca^{2+}]_i$ in either the presence or absence of external Ca^{2+} (Fig. 2D). These results suggested that LPC increases $[Ca^{2+}]_i$ in the cells by releasing Ca^{2+} from ER, and that CGA might be involved in inhibiting intracellular Ca^{2+} release from the ER.

Effect of CGA and SOC inhibitors on the LPS-induced increase in the intracellular Ca^{2+} concentration

Increased $[Ca^{2+}]_i$ might be induced by depletion of Ca^{2+} in the ER (14). To test this, cells were pretreated with the SOC blockers, Gd^{3+} (100 μmol/L) and La^{3+} (100 μmol/L), and then incubated with LPC (50 μmol/L) to measure $[Ca^{2+}]_i$. Gd^{3+} and La^{3+} completely ameliorated the increase in $[Ca^{2+}]_i$ induced by LPC (Fig. 3A). These results suggest that the $[Ca^{2+}]_i$ increase is induced by LPC in cells via SOCs and is suppressed by CGA treatment. To demonstrate the effect of the SOC inhibitors on cell viability, cells were pretreated with Gd^{3+} and La^{3+} for 30 minutes and then 30 μmol/L LPC was added. Both Gd^{3+} and La^{3+} prevented the LPS-induced reduction in cell viability and these blocking effects were similar to those of CGA (Fig. 3B). SOC channels are functionally involved in TRPC mRNA expression; therefore, we measured the expression levels of *TRPC* genes using reverse transcription polymerase chain reaction (RT-PCR) in HUVECs. *TRPC1* mRNA expression was increased by LPC treatment, and both CGA and SOC blockers suppressed *TRPC1* expression significantly (Fig. 3C). However, the expressions of other TRPC isoforms, *TRPC3* and *TRPC7*, were not changed significantly by LPC and SOC blockers (Fig. 3C). We then measured TRPC1 protein levels under the same conditions. The TRPC1 protein level was increased by LPC and decreased by SOC blockers in HUVECs (Fig.

3D). These findings indicated that CGA and SOC blockers ameliorated the expression of *TRPC1* induced by LPC in HUVECs.

Effect of CGA and SOC inhibitors on ROS generated by LPC

To evaluate whether LPC is involved in generating ROS in HUVECs, and whether this effect is suppressed by CGA, LPC (50 μmol/L) was administered to HUVECs and ROS levels were measured by fluorescent staining. ROS generation increased drastically in LPC-treated cells compared with that in the control group (Fig. 4). The LPC-mediated increases in ROS levels were suppressed by Gd^{3+} (100 μmol/L) and La^{3+} (100 μmol/L) compared with that in the LPC-treated cells. Moreover, CGA, as well as the ROS scavenger, N-acetyl-L-cysteine (NAC), decreased the ROS levels significantly (Fig. 4A). Finally, because ROS was induced by LPC, cells exposed to 50 μmol/L LPC were treated with 10 μmol/L diphenyleneiodonium (DPI), an NADPH oxidant inhibitor, and 10 μmol of rotenone, known as an inhibitor of phosphorylation in the mitochondrial electron transport system (ETS), respectively (Fig. 4B). Rotenone caused a more significant decrease in ROS than was observed using DPI. These data demonstrated that LPC might stimulate ROS generation in the mitochondria rather than in the cytoplasm.

DISCUSSION

Atherosclerosis is caused by hypercholesterolemia, smoking, hypertension, and diabetes. Increased levels of oxidized LDL (ox-LDL) in the cell is the most important factor in the development of atherosclerosis (15). LPC is a major component of ox-LDL, and is involved in the inflammatory response in cells, playing an important role in the development of atherosclerosis (16). The aim of this study was to evaluate the effects of LPC on $[Ca^{2+}]_i$, cell viability, and ROS generation in HUVECs, and to investigate the protective effect of CGA, including its mechanism of action. LPC treatment, known to induce cytotoxicity in endothelial

cells, reduced the viability of HUVECs in a dose-dependent manner, and CGA blocked this LPC-induced cytotoxicity.

LPC is a major causal factor in atherosclerosis, which triggers malfunction or inflammation of endothelial cells (17). Dysfunction of endothelial cells is closely related to oxidative stress caused by increased ROS production (18). Moreover, LPC causes endothelial cell dysfunction by increasing ROS-mediated oxidative stress (19). The increased $[Ca^{2+}]_i$ induced by LPC plays a central role in the initial process of cell injury (20). LPC challenge involves two phases in endothelial cells. The first is the initial rapid increase in $[Ca^{2+}]_i$ and the second is the continued maintenance of a high $[Ca^{2+}]_i$ concentration (21). U73122 and dantrolene-Na^+ treatment (inhibitors of IP3R and ryanodine receptors in the ER) reduced $[Ca^{2+}]_i$; therefore, the initial increase in $[Ca^{2+}]_i$ might be caused by release of Ca^{2+} from the ER (22). In addition, when extracellular Ca^{2+} was removed using up to 2 mmol/L EGTA (ethylene glycol-bis(β-aminoethyl ether)-N,N,N',N'-tetraacetic acid), the increased Ca^{2+} levels induced by LPC were not maintained and were restored to the basal state, indicating that the $[Ca^{2+}]_i$ might be dependent on extracellular Ca^{2+} (23). Thus, CGA suppresses Ca^{2+} influx from both the ER and the extracellular environment.

The non-selective cation channels SOCs are the main channels for Ca^{2+} influx in non-excitable cells during Ca^{2+} depletion from the ER (24). Gd^{3+} and La^{3+} are used as blocking agents of SOCs and transient receptor potential (TRP) pathways (25). Among TRPs, the canonical types of TRP (TRPC) channels are activated by phospholipase C (PLC) (26). If the signal molecules bind to G-protein-coupled receptors, the activity of PLC stimulates the decomposition of the phospholipid phosphatidylinositol 4,5-bisphosphate in the cell membrane into diacylglycerol and 1,4,5-tris-phosphate (IP3) (27). Gd^{3+} and La^{3+} reduced the expression of *TRPC1* (Fig. 3); therefore, SOC blockers might inhibit the activity of PLC, which inhibits IP3-mediated release of Ca^{2+} from the ER by inhibiting the generation of IP3. Similarly, like Gd^{3+}

and La^{3+}, CGA might also inhibit extracellular Ca^{2+} influx and LPC-induced release of Ca^{2+} from the ER.

Antioxidants comprise a variety of compounds that prevent damage to cells and tissues caused by generation of ROS and oxidative stress. The most well-known antioxidant is NAC, a synthetic precursor of glutathione (GSH) containing thiol (28). NAC produces an antioxidant effect by removing ROS through the increased generation of intracellular GSH (29). Among a number of antioxidants in nature, CGA is an polyphenol-containing antioxidant that has myocardial protective and anti-tumor effects; inhibits the oxidation of LDL and DNA through chelating metal ions; and can remove ROS (13). CGA also represses ROS production, the expression of adhesion molecules, and the adhesion of monocytes in HUVECs (30). In our study, LPC-induced increases in ROS were reduced by CGA treatment, as well as by NAC challenge (Fig. 4). Moreover, SOC blockers also suppressed ROS production in a manner similar to CGA. Thus, these results suggested that CGA acts as an antioxidant by inhibiting free radicals in HUVECs.

Usually, the generation of ROS occurs via three major pathways. The first is oxidative phosphorylation in the mitochondrial electron transport system (ETS), the second is the activation of NADPH oxidase, and the third is via the action of lipoxygenase (31). In this study, rotenone, rather than DPI, was shown to generate oxidative phosphorylation of the mitochondrial ETS in HUVECs. Thus, our data suggested that LPC induces ROS production through increased oxidative phosphorylation in the mitochondrial ETS. Ca^{2+} influx into cells is increased via SOC by ROS generated in hypoxic conditions (32). Moreover, ROS produced by mitochondria is associated with Ca^{2+} channels in the cardiovascular system (33). Thus, ROS are generated by an increase in $[Ca^{2+}]_i$, whereas the production of ROS affects Ca^{2+} influx into the cells. It has been hypothesized that there is a correlation between the increase in Ca^{2+} concentration and the generation of ROS in cells (33). If the increases in Ca^{2+} and ROS levels cause inflammation of

the cells, CGA might prevent atherosclerosis efficiently via its anti-inflammatory effect in vascular endothelial cells.

In this study, the Ca^{2+} level in LPC-treated cells was increased by releasing Ca^{2+} from the ER and by increasing Ca^{2+} influx via SOCs in HUVECs. In addition, we confirmed that TRPC1 was involved in the increased $[Ca^{2+}]_i$. LPC induced cytotoxicity and ROS generation in the mitochondrial ETS. CGA blocked production of ROS and Ca^{2+} intake via SOCs through decreased TRPC1 gene expression, resulting in inhibition of cell damage from ROS in HUVECs. A previous study demonstrated that *TRPC1* and *TRPC3* expression levels were regulated by activating Bax and caspase-3 and inhibiting Bcl-2 and pAkt in human coronary artery smooth muscle cells (SMCs) (34). However, they also suggested that TRPC3 did not participate in calcium-sensing receptor mediated calcium influx in HUVECs (11). Even though we did not demonstrate the molecular mechanism of CGA on TRPC1 gene expression, previous report suggested that caveolin-1, as a plasma membrane protein for the channel, interacts with TRPC channels to recruit and stabilize them in the plasma membrane (35). Thus, caveolin-1 might be a TRPC1 channel modulator. In summary, we demonstrated that CGA suppresses the generation of ROS and may be considered as a pharmaceutical agent to ameliorate atherosclerosis by preventing cell damage from ROS in HUVECs.

MATERIALS AND METHODS

Chemicals and reagents

Endothelial cell basal medium (EBM-2) for endothelial cell growth was purchased from Lonza (Walkersville, MD, USA). Trypsin EDTA was purchased from Gibco-Invitrogen (Grand Island, NY, USA). Intracellular Ca^{2+} was determined using the fura-2 acetoxymethyl (Fura-2/AM) ester from Molecular Probes (Eugene, OR, USA). Cell viability was determined using 3-(4,5-dimethylthiazol-2-yl)-2,5-diphenyltetrazolium bromide (MTT) from Sigma (St. Louis, MO, USA). 1-palmitoyl-sn-glycero-3-phosphocholine, chlorogenic acid, gadolinium (Gd^{3+}), lanthanum (La^{3+}), and all other reagents were also purchased from Sigma.

Cell culture

HUVECs were cultivated in EBM-2 media supplemented with 2 % fetal bovine serum, 0.4 % recombinant human fibroblast growth factor-B, 0.1 % recombinant human epidermal growth factor, 0.1 % recombinant human vascular endothelial growth factor, 0.1 % ascorbic acid, 0.1 % recombinant long R insulin-like growth factor-1, 0.1 % heparin, 0.1 % gentamicin sulfate amphotericin-B, and 0.04% hydrocortisone at 37 °C and 5 % CO_2.

Assessment of Cell Survival

The MTT calorimetric assay determines the ability of viable cells to convert a soluble tetrazolium salt (MTT) into an insoluble formazan precipitate. MTT, a water-soluble yellow dye that is readily taken up by viable cells, is reduced by the action of mitochondrial dehydrogenases. The reduction product is blue, and the water-insoluble formazan crystal that can be dissolved in an organic solvent for spectrophotometric determination of its concentration. Cells were seeded at a density of 3×10^4 cells/well in a 96-well culture plate and treated with or without protective material prior to exposure to LPC (30 μg/ml). MTT was then added to each well and incubated

for an additional 3 h at 37 °C. Subsequently, 100 µl of dimethyl sulfoxide was added to dissolve the reduced MTT and the absorbance at 570 nm was read on a microplate reader (Molecular Devices, Sunnyvale, CA, USA). Data are expressed as a percentage of the control, which was considered 100 % viable.

Reverse Transcription (RT)-PCR Analysis

Total RNA was isolated from cultured cells using the Trizol reagent (Invitrogen, Carlsbad, CA, USA). Total RNA was reverse-transcribed into cDNA using a reverse transcription kit (Promega, Madison, WI, USA) and oligo dT, which was then used for semi-quantitative RT-PCR. The generated cDNA was amplified by Emerald Amp PCR (Takara, Shiga, Japan) using the following primers: TRPC1 forward 5'-GATTTTGGAAAATTTCTTGGGATGT-3', reverse 5'-TTTGTCTTCATGATTTGCTATCA-3' (369 bp); TRPC3 forward 5'-GAC ATA TTC AAG TTC ATG GTC CTC-3', reverse 5'-ACA TCA CTG TCA TCC TCA ATT TC-3'(223 bp); TRPC7 forward 5'-CAG AAG ATC GAG GAC ATC AGC-3', reverse 5'-GTG CCG GGC ATT CAC GTG GTA-3'(304 bp); glyceraldehyde-3-phosphate dehydrogenase (GAPDH) forward 5'-CGTCTTCACCACCATGCAGA-3', and reverse 5'-CGCCCATCACGCCACAGTTT-3' (300 bp). PCR products were electrophoresed on a 1.2 % agarose gel and images were captured with a photo-documentation imaging system.

Detection of Intracellular ROS

To measure ROS, HUVECs were grown in 8-well plates at 4×10^4 cells/well and incubated for 30 min in the dark with 10 µmol/L 2',7'-dichlorofluorescein diacetate (Invitrogen). After a gentle rinse with PBS, the cells were fixed in 3.7% formaldehyde for 10 min. The cells were then washed with PBS and mounted with slowfade gold antifade reagent (Invitrogen). The ROS signal was detected using a confocal microscope (Carl Zeiss, Dublin, CA, USA), set to 485 nm

excitation and 535 nm emission.

Measurement of intracellular calcium concentration

Fluorescence measurements of $[Ca^{2+}]_i$ were performed as previously described (36). Briefly, coverslips containing HUVECs were loaded with the acetoxymethyl ester of fura-2/AM. Fura-2/AM (3 μM) in 1.8 mM Ca^{2+}-containing physiological saline solution (PSS; 1.8 mM $CaCl_2$, 5 mM KCl, 10 mM HEPES [pH 7.4], 1.2 mM $MgCl_2$, 126 mM NaCl, 0.2 % BSA, and 10 mM glucose) was added to the HUVECs at room temperature for 30 min, and then washed three times with dye-free saline for 30 min. Fluorescence was monitored using a dual-wavelength system (Intracellular Imaging, Cincinnati, OH, USA). The cells were excited at 340 and 380 nm, and the emission intensity at 510 nm was recorded. The data were expressed as the ratio of 510 nm emissions of fura-2 fluorescence obtained from excitation at 340 and 380 nm, respectively. For the Ca^{2+}-free solution, Ca^{2+} was removed from the solution and substituted with 2 mM EGTA.

Immunoblotting.

Total proteins were prepared from HUVECs and analyzed following a standard protocol. Anti-TRPC1 (ab51255; Abcam, Cambridge, MA) and anti-GAPDH (2118s; Cell Signaling Technology, Danvers, MA) were used as specific antibody. The bands were developed using ECL immunoblotting detection kit (Amersham Bioscience, Piscataway, NJ) and detected using an imager (Fusion FX; Vilber, Lourmat, Australia).

Statistical analyses

All data are expressed as the mean ± S.E.M. Values were compared using Predictive Analytics Software Statistics 18 (PASW Statistics 18, IBM Corporation, NY, USA), followed by

Student's t-test. $p < 0.05$ was regarded as statistically significant.

ACKNOWLEDGEMENTS

This study was supported financially by a National Research Foundation (NRF) Grant funded by the Korean Government (MSIP) (No. 2014R1A5A2010008 and NRF-2016R1A2B4008516) and the Korea New faculty, Korea Research Foundation (NRF-2013R1A1A1006606) to SS.

CONFLICT OF INTEREST

No potential conflicts of interest relevant to this article were reported.

REFERENCES

1. Grandl M and Schmitz G (2010) Fluorescent high-content imaging allows the discrimination and quantitation of E-LDL-induced lipid droplets and Ox-LDL-generated phospholipidosis in human macrophages. Cytometry A 77, 231-42.
2. Steinbacher P and Eckl P (2015) Impact of oxidative stress on exercising skeletal muscle. Biomolecules 5, 356-77.
3. Fedrizzi L, Lim D, Carafoli E (2008) Calcium and signal transduction. Biochem Mol Biol Educ 36, 175-80.
4. Brini M, Cali T, Ottolini D et al (2013) Intracellular calcium homeostasis and signaling. Met Ions Life Sci 12, 119-68.
5. Korkiamaki T, Yla-Outinen H, Leinonen P et al (2005) The effect of extracellular calcium concentration on calcium-mediated cell signaling in NF1 tumor suppressor-deficient keratinocytes. Arch Dermatol Res 296, 465-72.
6. Mak S, Sun H, Acevedo F et al (2010) Differential expression of genes in the calcium-signaling pathway underlies lesion development in the LDb mouse model of atherosclerosis. Atherosclerosis 213, 40-51.
7. Xu F, Ji J, Li L et al (2007) Activation of adventitial fibroblasts contributes to the early development of atherosclerosis: a novel hypothesis that complements the "Response-to-Injury Hypothesis" and the "Inflammation Hypothesis". Med Hypotheses 69, 908-12.
8. Bernatoniene J, Masteikova R, Majiene D et al (2008) Free radical-scavenging activities of Crataegus monogyna extracts. Medicina (Kaunas) 44, 706-12.
9. Maas M, Petereit F, Hensel A (2008) Caffeic acid derivatives from Eupatorium perfoliatum L. Molecules 14, 36-45.
10. Hicks JM, Muhammad A, Ferrier J et al (2012) Quantification of chlorogenic acid and hyperoside directly from crude blueberry (Vaccinium angustifolium) leaf extract by NMR spectroscopy analysis: single-laboratory validation. J AOAC Int 95, 1406-11.
11. Liang N and Kitts DD (2015) Role of Chlorogenic Acids in Controlling Oxidative and Inflammatory Stress Conditions. Nutrients 8.
12. Bonita JS, Mandarano M, Shuta D et al (2007) Coffee and cardiovascular disease: in vitro, cellular, animal, and human studies. Pharmacol Res 55, 187-98.

13. Kwon SH, Lee HK, Kim JA et al (2010) Neuroprotective effects of chlorogenic acid on scopolamine-induced amnesia via anti-acetylcholinesterase and anti-oxidative activities in mice. Eur J Pharmacol 649, 210-7.
14. Bogeski I, Bozem M, Sternfeld L et al (2006) Inhibition of protein tyrosine phosphatase 1B by reactive oxygen species leads to maintenance of Ca2+ influx following store depletion in HEK 293 cells. Cell Calcium 40, 1-10.
15. Choi KM (2016) The Impact of Organokines on Insulin Resistance, Inflammation, and Atherosclerosis. Endocrinol Metab (Seoul) 31, 1-6.
16. Matsumoto T, Kobayashi T, Kamata K (2007) Role of lysophosphatidylcholine (LPC) in atherosclerosis. Curr Med Chem 14, 3209-20.
17. Schmitz G and Ruebsaamen K (2010) Metabolism and atherogenic disease association of lysophosphatidylcholine. Atherosclerosis 208, 10-8.
18. Diano S (2013) Role of reactive oxygen species in hypothalamic regulation of energy metabolism. Endocrinol Metab (Seoul) 28, 3-5.
19. Liang GH, Park S, Kim MY et al (2010) Modulation of nonselective cation current by oxidized LDL and lysophosphatidylcholine and its inhibitory contribution to endothelial damage. Life Sci 86, 733-9.
20. Chen L, Liang B, Froese DE et al (1997) Oxidative modification of low density lipoprotein in normal and hyperlipidemic patients: effect of lysophosphatidylcholine composition on vascular relaxation. J Lipid Res 38, 546-53.
21. Kim MS, Hong JH, Li Q et al (2009) Deletion of TRPC3 in mice reduces store-operated Ca2+ influx and the severity of acute pancreatitis. Gastroenterology 137, 1509-17.
22. Mogami H, Lloyd Mills C, Gallacher DV (1997) Phospholipase C inhibitor, U73122, releases intracellular Ca2+, potentiates Ins(1,4,5)P3-mediated Ca2+ release and directly activates ion channels in mouse pancreatic acinar cells. Biochem J 324 (Pt 2), 645-51.
23. Ogita T, Tanaka Y, Nakaoka T et al (1997) Lysophosphatidylcholine transduces Ca2+ signaling via the platelet-activating factor receptor in macrophages. Am J Physiol 272, H17-24.
24. Burdakov D, Petersen OH, Verkhratsky A (2005) Intraluminal calcium as a primary regulator of endoplasmic reticulum function. Cell Calcium 38, 303-10.

25. Pena F and Ordaz B (2008) Non-selective cation channel blockers: potential use in nervous system basic research and therapeutics. Mini Rev Med Chem 8, 812-9.
26. Plant TD and Schaefer M (2003) TRPC4 and TRPC5: receptor-operated Ca2+-permeable nonselective cation channels. Cell Calcium 33, 441-50.
27. McLaughlin S and Murray D (2005) Plasma membrane phosphoinositide organization by protein electrostatics. Nature 438, 605-11.
28. Chen N, Aleksa K, Woodland C et al (2007) The effect of N-acetylcysteine on ifosfamide-induced nephrotoxicity: in vitro studies in renal tubular cells. Transl Res 150, 51-7.
29. Yamanaka T and Hishinuma A (1995) [Different effects of anticancer drugs on two human thyroid cell lines with different stages of differentiation]. Nihon Naibunpi Gakkai Zasshi 71, 73-86.
30. Liao Y, Dong S, Kiyama R et al (2013) Flos lonicerae extracts and chlorogenic acid protect human umbilical vein endothelial cells from the toxic damage of perfluorooctane sulphonate. Inflammation 36, 767-79.
31. Salmeen A and Barford D (2005) Functions and mechanisms of redox regulation of cysteine-based phosphatases. Antioxid Redox Signal 7, 560-77.
32. Wang YX and Zheng YM (2010) ROS-dependent signaling mechanisms for hypoxic Ca(2+) responses in pulmonary artery myocytes. Antioxid Redox Signal 12, 611-23.
33. Fearon IM (2006) OxLDL enhances L-type Ca2+ currents via lysophosphatidylcholine-induced mitochondrial reactive oxygen species (ROS) production. Cardiovasc Res 69, 855-64.
34. Wang Y, Wang Y, Li GR (2016) TRPC1/TRPC3 channels mediate lysophosphatidylcholine-induced apoptosis in cultured human coronary artery smooth muscles cells. Oncotarget 7, 50937-51.
35. Ong HL and Ambudkar IS (2015) Molecular determinants of TRPC1 regulation within ER-PM junctions. Cell Calcium 58, 376-86.
36. Yi FX, Magness RR, Bird IM (2005) Simultaneous imaging of [Ca2+]i and intracellular NO production in freshly isolated uterine artery endothelial cells: effects of ovarian cycle and pregnancy. Am J Physiol Regul Integr Comp Physiol 288, R140-8.

Figure legends

Fig. 1. Effects of chlorogenic acid (CGA) on lysophosphatidylcholine (LPC)-induced cell death in human umbilical vein endothelial cells (HUVECs). (A) Effects of LPC on cell viability in HUVECs. LPC treatment for 1 h decreased cell viability in a dose-dependent manner. (B) CGA attenuated the LPC-induced decrease in cell viability. Data are the mean ± SEM of three separate experiments. (C) Effects of CGA on HUVECs viability without LPC treatment. Treatment by CGA alone for 24 h significantly increases the cell viability. $^{**}p < 0.01$, $^{***}p < 0.001$ compared with the corresponding vehicle only control; $^{###}p < 0.001$ compared with the corresponding single treatment with 30 μmol/L LPC.

Fig. 2. Effects of lysophosphatidylcholine (LPC) on intracellular calcium concentration ($[Ca^{2+}]_i$) in human umbilical vein endothelial cells (HUVECs). (A) LPC increased $[Ca^{2+}]_i$ dose-dependently in a 1.8 mmol/L Ca^{2+} bathed-external solution. (B) The effects of LPC on $[Ca^{2+}]_i$ depend on the external Ca^{2+} in HUVECs. LPC induced only an initial transient peak of $[Ca^{2+}]_i$ in the absence of external Ca^{2+} and did not elicit the increase of $[Ca^{2+}]_i$ under treatment with endoplasmic reticulum blockers: 50 μmol/L dantrolene and 10 μmol/L U73122. The sustained $[Ca^{2+}]_i$ increase represents Ca^{2+} influx from the extracellular solution. (C) Effects of chlorogenic acid (CGA) on LPC-induced $[Ca^{2+}]_i$ in HUVECs. The CGA blocked the LPC-induced sustained $[Ca^{2+}]_i$ increase. (D) No effect of CGA without LPC in HUVECs. CGA (300 μmol/L and 1000 μmol/L) was treated without Ca^{2+} and with 1.8 mM Ca^{2+} in HUVECs. Data are the mean values of three independent experiments.

Fig. 3. Effects of store-operated channel (SOC) blockers on lysophosphatidylcholine (LPC)-induced $[Ca^{2+}]_i$ in human umbilical vein endothelial cells (HUVECs). (A) SOC blockers

inhibited the LPC-induced sustained $[Ca^{2+}]_i$ increase. (B) Comparative effects of chlorogenic acid (CGA) and SOC blockers on LPC-induced cell death in HUVECs. CGA increased cell survival to the same levels as the SOC blockers. (C) Inhibitory effects of CGA on LPC-induced expressions of transient receptor potential canonical (TRPC) channels 1, 3, and 7 in HUVECs. (D) Immunoblotting for the TRPC1 protein under treatment by CGA and SOC blockers in HUVECs. The bar graph shows that CGA significantly suppressed LPC-induced TRPC1 mRNA expression with similar potency to gadolinium (Gd^{3+}) and lanthanum (La^{3+}). PCR data normalized to GAPDH are expressed as the mean values of three separate experiments. $^{**}p < 0.01$, $^{***}p < 0.001$ compared with a corresponding single treatment with the vehicle control; $\#p < 0.05$, $\#\#p < 0.01$, $\#\#\#p < 0.001$ compared with a corresponding single treatment with 30 μmol/L LPC.

Fig. 4. Effects of chlorogenic acid (CGA) and store-operated channel (SOC) blockers on lysophosphatidylcholine (LPC)-induced ROS generation in human umbilical vein endothelial cells (HUVECs). (A) LPC increased ROS generation. CGA or SOC blockers decreased the LPC-induced ROS generation with a similar potency to N-acetyl-L-cysteine (NAC). The bar graph shows that CGA decreased the LPC-induced ROS generation with the same efficiency as a ROS generation inhibitor or SOC blockers gadolinium (Gd^{3+}) and lanthanum (La^{3+}) (B) Effects of ROS generation inhibitors on LPC-induced ROS generation in HUVECs. Rotenone inhibited LPC-induced ROS generation. The bar graph shows that rotenone decreased LPC-induced ROS generation to a greater extent than diphenyleneiodonium (DPI). Data are the mean ± SEM of three separate experiments. $^{**}p < 0.01$ compared with a corresponding single treatment with the vehicle control; $\# p < 0.05$, $\#\# p < 0.01$ compared with a corresponding single treatment with 50 μmol/L LPC.

Figures

Jung HJ et al. Fig. 1.

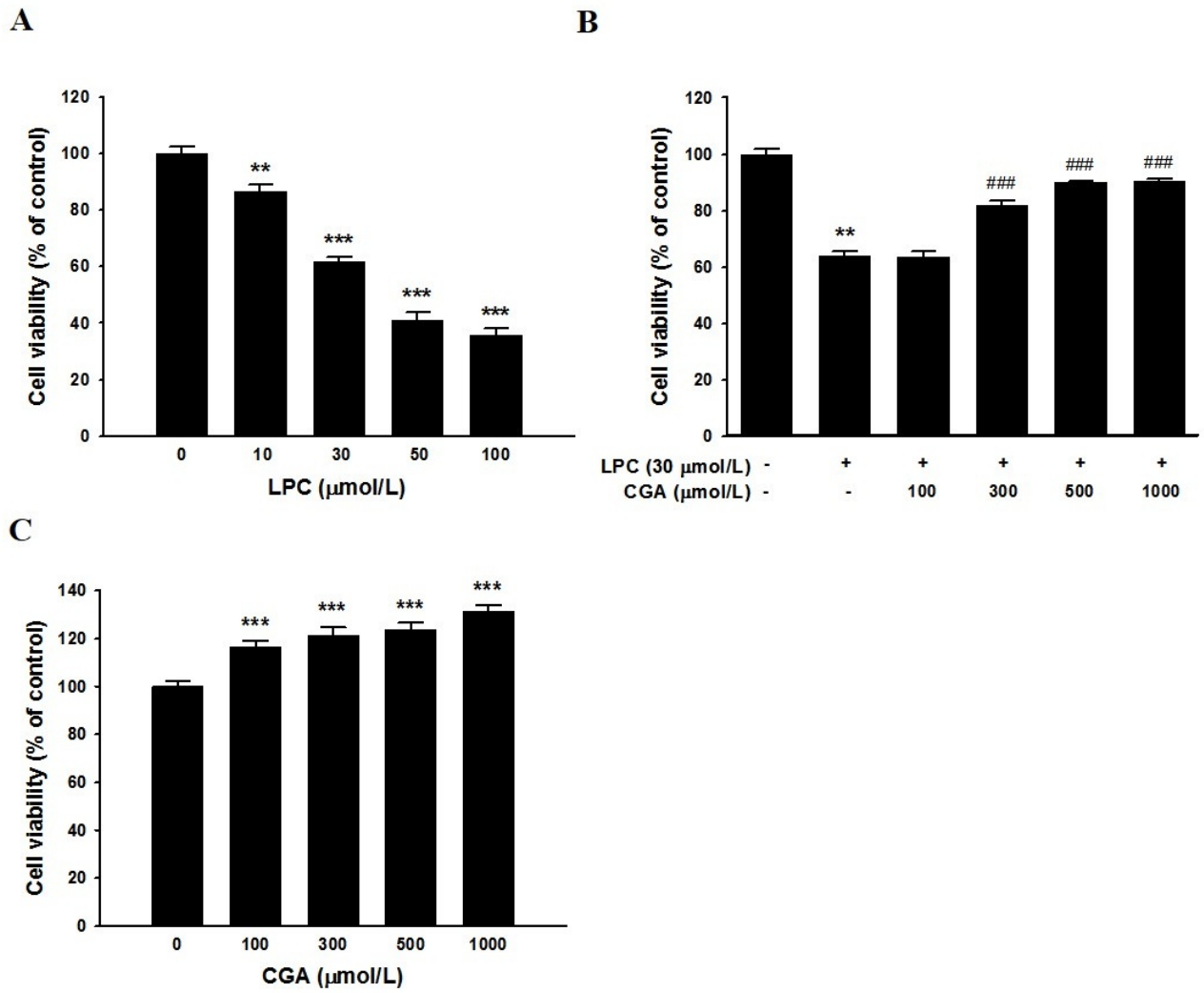

Jung HJ et al. Fig. 2.

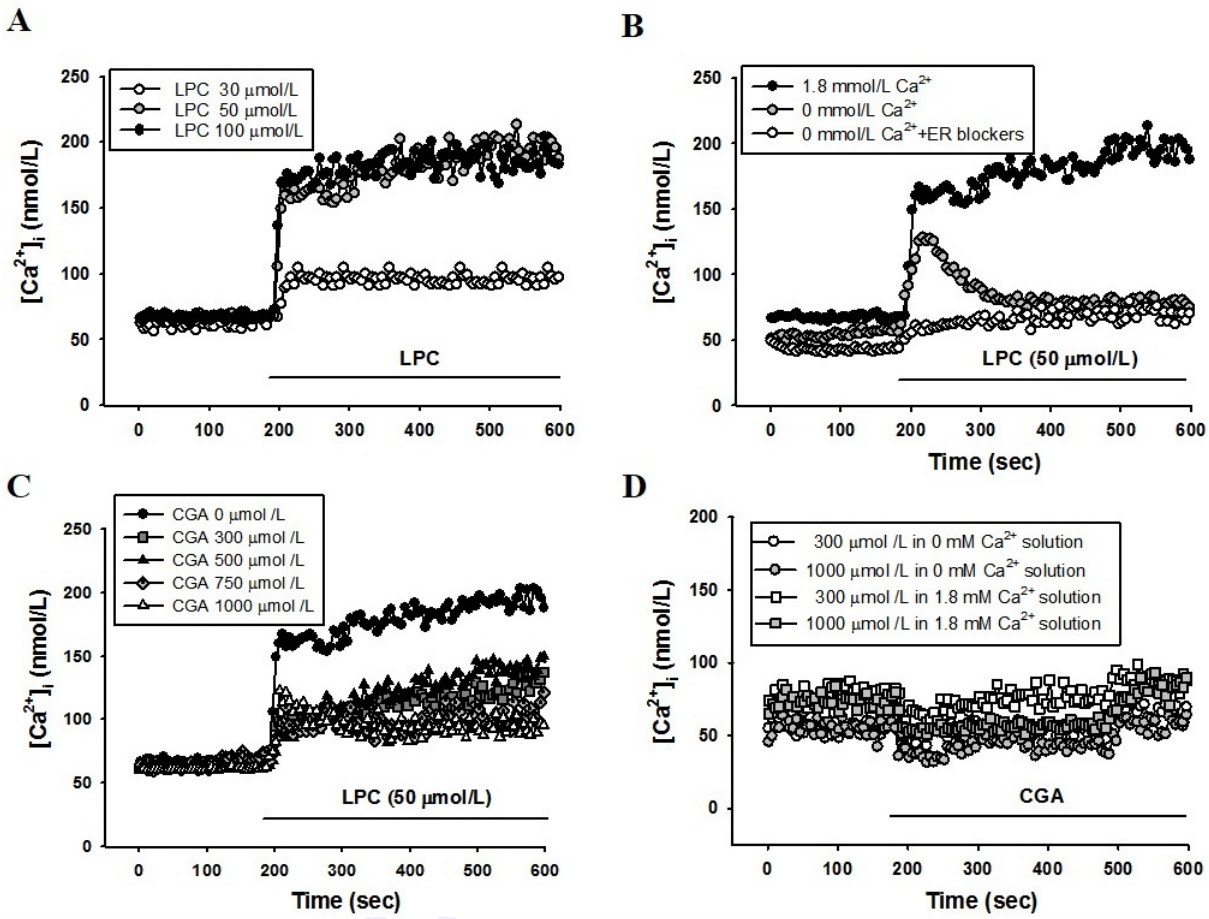

Jung HJ et al. Fig. 3.

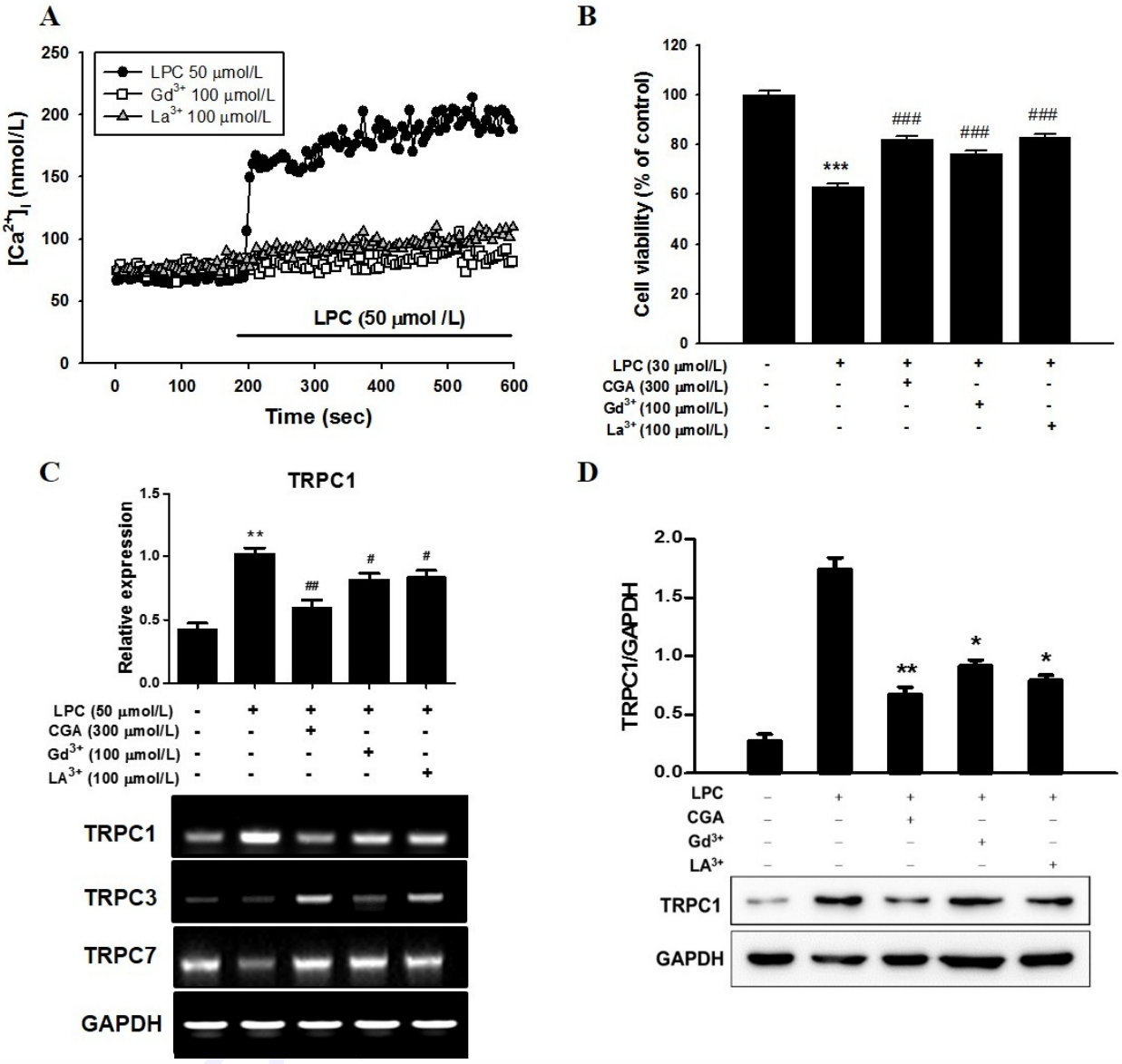

Jung HJ et al. Fig. 4.